HHS Public Access

Author manuscript

Curr Opin Biomed Eng. Author manuscript; available in PMC 2018 September 01.

Published in final edited form as:

Curr Opin Biomed Eng. 2017 September ; 3: 20–27. doi:10.1016/j.cobme.2017.09.009.

Computer-aided diagnosis of prostate cancer with MRI

Baowei Fei

Department of Radiology and Imaging Sciences, Emory University School of Medicine, Atlanta, GA 30329, USA

The Wallace H. Coulter Department of Biomedical Engineering, Emory University and Georgia Institute of Technology, Atlanta, GA 30329, USA

Department of Mathematics and Computer Science, Emory College of Emory University, Atlanta, GA 30329, USA

Winship Cancer Institute of Emory University, Atlanta, GA 30329, USA

Abstract

Multi-parametric magnetic resonance imaging (mp-MRI) has an increasingly important role in the diagnosis of prostate cancer. Due to the large amount of data and variations in mp-MRI, tumor detection can be affected by multiple factors, such as the observer's clinical experience, image quality, and appearance of the lesions. In order to improve the quantitative assessment of the disease and reduce the reporting time, various computer-aided diagnosis (CAD) systems have been designed to help radiologists identify lesions. This manuscript presents an overview of the literature regarding prostate CAD using mp-MRI, while focusing on the studies of the most recent five years. Current prostate CAD technologies and their utilization are discussed in this review.

Introduction

Prostate cancer (PCa) is currently the most common cancer occurring in men and is a leading cause of cancer-related deaths among men in the United States [1]. In 2017, it is estimated that the number of new cases and deaths will be 161,360 and 26,730, respectively, and thus accounting for 19.3% of the new cancer cases and 8.4% of the cancer deaths in American men [1]. Currently, the clinical standard for the definitive diagnosis of prostate cancer is transrectal ultrasound (TRUS)-guided sextant or systematic biopsy. However, this type of TRUS-guided biopsy has a significant sampling error and can miss up to 30% of cancers. [2] Several approaches have been investigated in order to improve the accuracy of image-guided prostate biopsy, including in-bore magnetic resonance imaging (MRI)-guided, cognitive fusion, and MRI/TRUS fusion-guided biopsy [3].

*Corresponding author: Baowei Fei, Ph.D., Department of Radiology and Imaging Sciences Emory University School of Medicine, 1841 Clifton Road NE, Atlanta, GA 30329, bfei@emory.edu, Phone: 404-712-5649, Website: www.fei-lab.org.

Multi-parametric MRI (mp-MRI) has an increasing role in the diagnosis of prostate cancer [4]. Mp-MRI provides excellent soft-tissue contrast and is clinically used for the detection, localization, characterization, staging, biopsy guidance, and active surveillance of prostate cancer. Mp-MRI includes T2-weighted (T2w) MRI, diffusion-weighted imaging (DWI), dynamic contrast-enhanced MRI (DCE-MRI), and MR spectroscopy (MRS). Mp-MRI has proven to be an effective technique for localizing high-risk prostate cancer [5,6]. It can also help to guide biopsies in order to achieve a higher tumor detection rate and better reflect the true Gleason grade. The European Society of Urogenital Radiology (ESUR) established the Prostate Imaging-Reporting and Data System (PI-RADS) scoring system for mp-MRI of the prostate [7]. Due to the large amount of mp-MRI data and the variations in MR scanners, sequences, protocols, and patient motion, and etc., the detection can be affected by multiple factors such as observer variability as well as the visibility and complexity of the lesions.

As mp-MRI creates large amounts of image data, computer-aided diagnosis of prostate cancer using mp-MRI has become an active area of research [8]. Although guidelines, such as the PI-RADS classification, exist for tumor detection and staging, no such guidelines are available for tumor delineation. Inter-observer studies show substantial variation in tumor contours [4,9]. CAD systems may help to make a clinical decision in a fast, effective, and reliable way. It may also improve the quantitative assessment of the disease. Currently, most CAD systems using prostate MRI focus on local, suspicious lesions and discrimination between benign and malignant lesions within the entire grand. In this manuscript, we discuss recent CAD research systems with prostate mp-MRI and their utilizations for prostate cancer diagnosis.

CAD systems and technologies for prostate MRI

Prostate CAD with MRI has evolved during the past 10 years. Lemaitre *et al.* [10] reported a comprehensive review of various technical aspects of prostate CAD with mp-MRI. Wang *et al.* [9] reviewed the CAD techniques related to image segmentation, registration, feature extraction, and classification. They listed the performances of 15 CAD systems. Various image processing and quantification methods were developed to facilitate prostate CAD with mp-MRI [11–21]. To increase the robustness of the interpretation of mp-MRI data, Rouviere *et al.* [22] showed that the combinations of shape and signal abnormalities in mp-MRI could be used to stratify the risk of malignancy of focal abnormalities in the prostate. Several alternative methods have been proposed to extract relevant features for each voxel for classification into normal and tumor tissue using basic classifiers. such as support vector machines [23] and logistic regression [24–26]. Viswanath *et al.* [27] use texture features, such as Gabor wavelet and Haar wavelet transformation extracted from the T2w-MRI scan, to represent each voxel. Groenendaal *et al.* [24] represent each voxel by several local statistics, e.g. minimum, maximum, and median of the intensities obtained on apparent diffusion coefficient (ADC) and Ktrans maps. Another approach is to detect regions of interest in the prostate using clustering [28]. Vos *et al.* [29] used a two-step approach based on a combination of features from T2w, T1, pharmacokinetic, and ADC maps. Texture features, such as blobness, were also used to improve its performance of CAD systems. The following section highlights several CAD systems and their technologies.

Giannini *et al.* presented a fully automatic CAD system [30]. The pipeline of the CAD system is shown in Figure 1; it is conceived as a 2-stage process. First, a malignancy probability map for all voxels within the prostate is created. A parametric. color-coded map of the prostate gland is generated; colors are assigned to the map based on the probability of each voxel to be cancerous. A candidate segmentation step is then performed to highlight suspected areas, thus evaluating both the sensitivity and the number of false-positive (FP) regions detected by the system. Training and testing of the CAD scheme is performed using whole-mount histological sections as the reference standard. In a cohort of 56 patients, the area under the ROC curve obtained during the voxel-wise step was 0.91, while, in the second step, a per-patient sensitivity of 97% was reached, with a median number of FP equal to 3 in the entire prostate. The system could be potentially used as the first or second reader in order to manage patients suspected of having PCa, and thus reducing both the radiologist's reporting time and the inter-reader variability.

Peng *et al.* evaluated the utility of a number of parameters obtained at T2w, DWI, and DCE-MRI for prostate CAD and assessment of cancer aggressiveness [31]. The 10^{th} percentile and average ADC values, T2w signal intensity histogram skewness (Figure 2), and Tofts K(trans) were analyzed, both individually and combined, via linear discriminant analysis, and with receiver operating characteristic curve analysis with AUC as the figure of merit, in order to distinguish cancer foci from normal foci. The Spearman rank-order correlation (rho) was calculated between the cancer foci Gleason score (GS) and image features. The study shows that the combination of 10^{th} percentile ADC, average ADC, and T2-weighted skewness yielded an AUC value for the same task of 0.95±0.02. ADC image features and K(trans) moderately correlate with the Gleason score.

Shah *et al.* developed a decision support system for detecting and localizing peripheral zone prostate cancers by using a machine learning approach to calculate a cancer probability map from mp-MRI [28]. Cancer and normal regions were identified in the peripheral zone by correlating them to the whole-mount histology slides of the excised prostatectomy specimens. To facilitate the correlation, tissue blocks matching the MR slices were obtained using an MRI-based, patient-specific mold. Segmented regions on the MP-MRI were correlated to histopathology and used as training sets for the learning system that generated the cancer probability maps. Leave-one-patient-out cross-validation on the cancer and normal regions was performed to determine the learning system's efficacy, a genetic algorithm was used to find the optimal values for a set of parameters, and finally a cancer probability map was generated. This DSS provides a cancer probability map for peripheral zone prostate tumors based on endorectal mp-MRI (Figure 3).

Different CAD systems have their unique approaches for feature extraction and classification. Betrouni *et al.* reported an automatic framework for computer-aided analysis of mp-MRI of the prostate [32]. An unsupervised fusion scheme was described to analyze mp-MRI. This framework was not designed for cancer detection or characterization, but rather as a tool to assist radiologists in analyzing multisource data. Langer *et al.* developed a multi-parametric model suitable for prospectively identifying prostate cancer in the peripheral zone using mp-MRI [25]. The model uses the apparent diffusion coefficient (ADC), T2, the volume transfer constant (K(trans)), and the extravascular extracellular

volume fraction to map a PZ tumor. Litjens described a fully automated CAD system which consists of two stages [33]. In the first stage, we detect the initial candidates using multi-atlas-based prostate segmentation, voxel feature extraction, classification, and local maxima detection. The second stage segments the candidate regions, and using classification we obtain cancer likelihoods for each candidate. The features represent pharmacokinetic behavior, symmetry, appearance, etc. Niaf *et al.* reported a CAD system [34] which was based on a feature set derived from grey-level images, including first-order statistics, Haralick features, gradient features, semi-quantitative and quantitative (pharmacokinetic modelling) dynamic parameters, and four kinds of classifiers which were trained and compared, i.e. nonlinear support vector machine (SVM), linear discriminant analysis, k-nearest neighbors, and naive Bayes classifiers. Based on the t-test, mutual information, and minimum-redundancy-maximum-relevancy criteria, they compared a set of feature selection methods.

CAD systems may only use two of the multiple mp-MRI data, such as T2w and DWI [35], or T2w and DCE-MRI [36]. Kwak *et al.* proposed a CAD system [35] for prostate cancer to aid in improving the accuracy, reproducibility, and standardization of mp-MRI. The system utilizes T2w MRI, DWI, and texture features based on local binary patterns. The authors included a total of 244 patients, of which 108 patients were used for the CAD training. In distinguishing cancer from MR-positive, benign lesions, an area under the receiver operating characteristic curve (AUC) of 0.83 was achieved. For cancer vs MR-positive or MR-negative, benign lesions, the authors obtained an AUC of 0.89. The performance of the CAD system was not dependent on the specific regions of the prostate, e.g. a peripheral zone or transition zone. Vos *et al.* presented an approach for computer-assisted analysis of prostate lesions by combining information from T2w and DCE T1-w MRI [36]. Their study demonstrated a simple T2 estimation method with a diagnostic performance such that it complements a DCE, T1w-based, CAD system in discriminating malignant lesions from normal and benign regions.

Some CAD systems only use T2w MRI data. Rampun *et al.* reported a prostate CAD system based on T2w MRI [37] and suggested a set of discriminant texture descriptors extracted from T2w MRI data from which 215 texture descriptors were extracted and 11, different classifiers were used to achieve the best possible results. The method was tested based on 418, T2-weighted MR images taken from 45 patients and evaluated using nine-fold cross validation with five patients in each fold. The CAD system achieved an area under the receiver operating curve values equal to 90.0%±7.6%. Zhao *et al.* proposed a CAD system [38] that uses 12, quantitative image features extracted from prostate T2w MRI. The importance of each feature in cancer identification was compared in the peripheral zone (PZ) and the central gland (CG), respectively. The performance of the computer-aided diagnosis system supported by an artificial neural network was tested. Ten of 12 features had a significant difference ($P<0.01$) between PCa and non-PCa in the PZ.

Other CAD systems only use DCE-MRI data. Sung *et al.* reported a CAD system based DCE-MRI [39]. The perfusion parameters included baseline and peak signal intensities, the initial slope, maximum slope within the initial 50 seconds after the contrast injection (slope(50)), wash-in rate, washout rate, time to peak, percentage of relative enhancement,

percentage enhancement ratio, time of arrival, efflux rate constant from the extravascular extracellular space to the blood plasma, first-order rate constant for eliminating gadopentetate dimeglumine from the blood plasma, and constant depending on the properties of the tissue and represented by the size of the extravascular extracellular space. DCE-MRI examinations of 42 patients with prostate cancer were used to generate perfusion parameters. CAD for cancer detection was established by comprehensive evaluation of the parameters using a support vector machine. The results shows that CAD can improve the diagnostic performance of DCE-MRI in prostate cancer detection, which may, however, vary according to the zonal anatomy. Puech *et al.* developed CAD software for prostate cancer detection using DCE T1w MRI [40]. They designed a standardized, 5-level cancer suspicion score. After reviewing the MR images, radiologists established a diagnosis of suspicious areas based on the data of post-MRI transrectal ultrasound-guided biopsies. Their results suggest that the CAD system may improve radiologists' performances in prostate cancer identification, especially when they do not specialize in prostate imaging.

Proton magnetic resonance spectroscopic imaging (MRSI) has also been used for prostate CAD. Matulewicz *et al.* proposed an approach to assess whether an artificial neural network (ANN) model is a useful tool for automatic detection of cancerous voxels in the prostate from (1)H-MRSI datasets and whether the addition of information regarding anatomical segmentation improves the detection of cancer [41]. Their study demonstrates that automatic analysis of prostate MRSI to detect cancer using an ANN model is feasible and that application of anatomical segmentation from MRI as an additional input to ANN improves the accuracy of detecting cancerous voxels on MRSI.

Utilization of CAD with prostate MRI

Multiple studies have demonstrated the utility of CAD for prostate cancer diagnosis along with mp-MRI. First, CAD was able to improve the sensitivity, as reported in a recent study [42]. Giannini *et al.* compared the performance of clinically experienced readers for detecting prostate cancer using the likelihood map of the entire prostate, which was generated by a CAD system, with that of unassisted interpretation of mp-MRI [42]. Three, clinically experienced radiologists reviewed mp-MRI prostate cases twice. Readers first observed CAD marks on a likelihood map and classified as positive those suspicious for cancer. After six weeks, radiologists interpreted mp-MRI examinations unassisted, using their favorite protocol. Sensitivity, specificity, reading time, and inter-observer variability were compared for the two reading paradigms. The sensitivity was significantly higher with CAD for lesions with a Gleason score > 6 (91.3% vs 81.2%) or diameter >/=10 mm (95.0% vs 80.0%). The specificity was not affected by CAD. The average reading time when using CAD was significantly lower (220 s vs 60 s). This study by Giannini *et al.* demonstrated that with CAD, sensitivity increases and that CAD significantly reduces the reporting time of mp-MRI.

Second, CAD, such the system by Niaf *et al.* [43], improves the specificity. Their study assessed the impact of a CAD system on the characterization of focal prostate lesions using mp-MRI [43]. Twelve readers assessed the likelihood of malignancy of 88, predefined peripheral zone lesions using a five-level (0–4), subjective score (SS) in Reading Session 1.

This was repeated five weeks later in Reading Session 2. The CAD results were then disclosed and in Reading Session 3 the readers could amend the scores assigned during Reading Session 2. The diagnostic accuracy was assessed using an ROC regression model and was quantified according to the area under the ROC curve (AUC). Seven readers improved their performance between Reading Sessions 1 and 2, and all of the 12 readers improved their performance between Reading Sessions 2 and 3. For an SS positivity threshold of 3, the specificity of Reading Session 2 (79.0%) was significantly lower than that of Session 3 (86.2%). Niaf's study demonstrates that a CAD system improves the characterization of prostate lesions on mp-MRI by increasing the reading specificity.

Third, CAD can help less clinically experienced readers and can reach similar performance levels as those of clinically experienced observers [44]. Hambrock *et al.* investigated the effect of CAD on both less and more clinically experienced observer performance in the differentiation of benign from malignant prostate lesions on mp-MRI [44]. Six radiologists who were less clinically experienced regarding prostate imaging and four radiologists who were more experienced regarding prostate imaging were asked to characterize different regions suspicious for cancer as benign or malignant on mp-MRI first without and subsequently with CAD assistance. Stand-alone CAD had an overall AUC of 0.90. Without CAD, less clinically experienced observers had an overall AUC of 0.81, and which significantly increased to 0.91 with CAD. For clinically experienced observers, the AUC without CAD was 0.88, and which significantly increased to 0.91 with CAD. This study by Hambrock *et al.* demonstrated that the addition of CAD significantly improved the performance of less clinically experienced observers in distinguishing benign from malignant lesions, and when less clinically experienced observers used CAD, they achieved similar performance to that of clinically experienced observers. The stand-alone performance of CAD was similar to the performance of clinically experienced observers. In another study by Litjens *et al.* [33], it was demonstrated that an automated CAD system does not perform significantly differently from radiologists. Niaf *et al.* evaluated a CAD system for determining a likelihood measure of the presence of prostate cancer in the peripheral zone (PZ), based on mp-MRI [34]. Their study showed that the CAD scheme mimicked, in terms of AUC, the human experts in differentiating malignant from suspicious tissue, and thus demonstrating its potential for assisting in cancer identification in the PZ.

Fourth, CAD improves the differentiation between indolent and aggressive cancer [45]. Litjens *et al.* also investigated the added value of CAD to the diagnostic accuracy of PI-RADS reporting and the assessment of cancer aggressiveness [45]. Their study included MRI and the histopathological outcome of MR-guided biopsies of 130 patients. All cases were prospectively PI-RADS reported, and the reported lesions underwent CAD analysis. Logistic regression combined the CAD prediction and the radiologist PI-RADS score into a combination score. Receiver-operating characteristic (ROC) analysis and Spearman's correlation coefficient were used to assess the diagnostic accuracy and correlation to the cancer grade. The area-under-the-ROC-curve of the combination score was significantly higher than for the PI-RADS score of the radiologist (benign vs. cancer, 0.88 vs. 0.81 and indolent vs. aggressive, 0.88 vs. 0.78). The combination score correlated significantly stronger with the cancer grade (0.69) than with the individual CAD system or the radiologist (0.54 and 0.58). This study Litjens *et al.* demonstrated that i) CAD helps radiologists

discriminate benign findings from cancer in prostate MRI, ii) Combining PI-RADS and CAD improves the differentiation between indolent and aggressive cancer, and iii) Adding CAD to PI-RADS increases the correlation coefficient with respect to the cancer grade. These studies demonstrate the full potential of CAD technologies for the diagnosis of prostate cancer using mp-MRI.

Discussions and Conclusions

Mp-MRI is emerging as a powerful tool to diagnose and stage prostate cancer. However, its interpretation is a time-consuming and complex task requiring dedicated radiologists. A computer-aided diagnosis technique could allow quantitative integration of data derived from the different MRI sequences in order to obtain accurate, reproducible information useful for identifying and staging prostate cancer. There is a growing need to localize prostate cancers on mp-MRI in order to facilitate the use of image-guided biopsy, focal therapy, and active surveillance follow-up. Various studies [33,45–47] based on mp-MRI have shown that combining different features from different imaging modalities can increase CAD performance. Recently developed CAD systems for prostate mp-MRI were shown to have a similar diagnostic accuracy to that of well-trained prostate MR radiologists. Computer-aided systems may help physicians to obtain a fast, cost-effective, and more reproducible prostate cancer diagnosis from complex mp-MRI data.

Various reference standards were used for the validation of prostate CAD technologies. First, whole-mount, histopathological sections are the gold standard for the validation of CAD systems, as reported by multiple research groups [25,28,30,41]. Cancer and normal regions were identified on whole-mount histologic slides of the excised prostatectomy specimens and were then correlated with the lesions from their CAD systems using mp-MRI. To facilitate the correlation, tissue blocks matching the MR slices were obtained using an MR-based, patient-specific mold [28]. Second, standard histopathology from prostatectomy was also used as the reference standard for the validation [31,34,41,44]. Third, MR-guided biopsy was also used as the reference standard for CAD validation [33].

Prostate CAD with mp-MRI can have many applications. Cancer probability maps from CAD systems can potentially aid radiologists in accurately localizing peripheral-zone prostate cancers for planning targeted biopsies, focal therapy, and follow-up for active surveillance [28]. For radiotherapy of prostate cancer, MRI is being increasingly used for delineation of the prostate gland. For focal treatment of low-risk prostate cancer or focal-dose escalation for intermediate and high-risk cancer, tumor delineation is also required. With mp-MRI it becomes feasible to revisit the GTV-CTV concept during radiotherapy of prostate cancer. While detection of index lesions is quite reliable, contouring variability and the low sensitivity to small lesions suggest that the remainder of the prostate should be treated as CTV. Clinical trials that investigate the options for dose differentiation, for example with dose escalation to the visible tumor or dose reduction to the CTV, are therefore warranted [48]. Prostate CAD with mp-MRI could also be used to help radiologists in establishing the MRI-guided biopsy target [30].

Different studies used different technical approaches, such as field strengths, MR sequences, and use of an endorectal coil, for specific clinical indications. Prostate diagnosis with mp-MRI can be affected by multiple factors, such as observer variability and visibility and complexity of the lesions. Reported accuracies of the separate and combined mp-MRI techniques may vary for diverse clinical prostate cancer indications [4]. With the current mp-MRI technology, it is difficult to distinguish prostate cancer from confounders such as benign prostatic hyperplasia (BPH), post-biopsy hemorrhage, and atrophy [4,49]. The education and clinical experience of specialist radiologists are critical for accurate interpretation of mp-MRI findings and for the utilization of prostate CAD systems.

Although various studies have shown promising results demonstrating the additional value of CAD in prostate cancer diagnosis and staging, its integration into routine clinical practice still requires significant future efforts in optimizing workflows and meeting regulatory requirements. For example, results showed that a significant increase in diagnostic performance can be achieved when combining the radiologist PI-RADS score and the CAD system likelihood into a combination score [45]. This combination might not be feasible in clinical practice, as radiologists or urologists will always have the final say [45]. Research regarding computer-aided systems specifically focused for prostate cancer is a relatively new technology [10]. Currently, the results of most studies have been based on a relatively small number of patients. The use of CAD in conjunction with the radiologist for accurately characterizing prostate lesions is to be further investigated and clinical validated in order to provide a CAD system for decision support.

Acknowledgments

This work was partially supported by NIH grants CA156775, CA176684, and CA204254, and by the Georgia Research Alliance Distinguished Scientists Award.

References and recommended reading

Manuscripts of particular interest, published within the period of review, have been highlighted as:

● of special interest

●● of outstanding interest

1. Siegel RL, Miller KD, Jemal A. Cancer Statistics, 2017. CA Cancer J Clin. 2017; 67:7–30. [PubMed: 28055103]
2. Hricak H. MR imaging and MR spectroscopic imaging in the pre-treatment evaluation of prostate cancer. Br J Radiol. 2005; 78:S103–S111. [PubMed: 16306632]
3. Brown AM, Elbuluk O, Mertan F, Sankineni S, Margolis DJ, Wood BJ, Pinto PA, Choyke PL, Turkbey B. Recent advances in image-guided targeted prostate biopsy. Abdom Imaging. 2015; 40:1788–1799. [PubMed: 25596716]
4. Hoeks CM, Barentsz JO, Hambrock T, Yakar D, Somford DM, Heijmink SW, Scheenen TW, Vos PC, Huisman H, van Oort IM, et al. Prostate cancer: multiparametric MR imaging for detection, localization, and staging. Radiology. 2011; 261:46–66. [PubMed: 21931141]
5. Puech P, Rouviere O, Renard-Penna R, Villers A, Devos P, Colombel M, Bitker MO, Leroy X, Mege-Lechevallier F, Comperat E, et al. Prostate cancer diagnosis: multiparametric MR-targeted biopsy with cognitive and transrectal US-MR fusion guidance versus systematic biopsy–prospective multicenter study. Radiology. 2013; 268:461–469. [PubMed: 23579051]

6. Lawrence EM, Tang SY, Barrett T, Koo B, Goldman DA, Warren AY, Axell RG, Doble A, Gallagher FA, Gnanapragasam VJ, et al. Prostate cancer: performance characteristics of combined T(2)W and DW-MRI scoring in the setting of template transperineal re-biopsy using MR-TRUS fusion. Eur Radiol. 2014; 24:1497–1505. [PubMed: 24744197]
7. Barentsz JO, Richenberg J, Clements R, Choyke P, Verma S, Villeirs G, Rouviere O, Logager V, Futterer JJ. ESUR prostate MR guidelines 2012. Eur Radiol. 2012; 22:746–757. [PubMed: 22322308]
8●. Liu L, Tian Z, Zhang Z, Fei B. Computer-aided Detection of Prostate Cancer with MRI: Technology and Applications. Acad Radiol. 2016; 23:1024–1046. The authors provided a comprehensive review regarding computer-aided detection of prostate cancer using MRI, including the technology and applications. [PubMed: 27133005]
9. Wang S, Burtt K, Turkbey B, Choyke P, Summers RM. Computer aided-diagnosis of prostate cancer on multiparametric MRI: a technical review of current research. Biomed Res Int. 2014; 2014:789561. [PubMed: 25525604]
10. Lemaitre G, Marti R, Freixenet J, Vilanova JC, Walker PM, Meriaudeau F. Computer-Aided Detection and diagnosis for prostate cancer based on mono and multi-parametric MRI: a review. Comput Biol Med. 2015; 60:8–31. [PubMed: 25747341]
11. Viswanath S, Bloch BN, Rosen M, Chappelow J, Toth R, Rofsky N, Lenkinski R, Genega E, Kalyanpur A, Madabhushi A. Integrating Structural and Functional Imaging for Computer Assisted Detection of Prostate Cancer on Multi-Protocol In Vivo 3 Tesla MRI. Proc SPIE Int Soc Opt Eng. 2009; 7260:72603I.
12. Xiao G, Bloch BN, Chappelow J, Genega EM, Rofsky NM, Lenkinski RE, Tomaszewski J, Feldman MD, Rosen M, Madabhushi A. Determining histology-MRI slice correspondences for defining MRI-based disease signatures of prostate cancer. Comput Med Imaging Graph. 2011; 35:568–578. [PubMed: 21255974]
13. Tian Z, Liu L, Zhang Z, Xue J, Fei B. A supervoxel-based segmentation method for prostate MR images. Med Phys. 2017; 44:558–569. [PubMed: 27991675]
14. Tian Z, Liu L, Zhang Z, Fei B. Superpixel-Based Segmentation for 3D Prostate MR Images. IEEE Trans Med Imaging. 2016; 35:791–801. [PubMed: 26540678]
15. Tian Z, Liu L, Fei B. A supervoxel-based segmentation method for prostate MR images. Proc SPIE Int Soc Opt Eng. 2015; 9413
16. Tian Z, Liu L, Fei B. A fully automatic multi-atlas based segmentation method for prostate MR images. Proc SPIE Int Soc Opt Eng. 2015; 9413
17. Fei B, Duerk JL, Sodee DB, Wilson DL. Semiautomatic nonrigid registration for the prostate and pelvic MR volumes. Acad Radiol. 2005; 12:815–824. [PubMed: 16039535]
18. Fei B, Duerk JL, Boll DT, Lewin JS, Wilson DL. Slice-to-volume registration and its potential application to interventional MRI-guided radio-frequency thermal ablation of prostate cancer. IEEE Trans Med Imaging. 2003; 22:515–525. [PubMed: 12774897]
19. Fei B, Kemper C, Wilson DL. A comparative study of warping and rigid body registration for the prostate and pelvic MR volumes. Comput Med Imaging Graph. 2003; 27:267–281. [PubMed: 12631511]
20. Fei B, Duerk JL, Wilson DL. Automatic 3D registration for interventional MRI-guided treatment of prostate cancer. Comput Aided Surg. 2002; 7:257–267. [PubMed: 12582978]
21. Fei B, Wheaton A, Lee Z, Duerk JL, Wilson DL. Automatic MR volume registration and its evaluation for the pelvis and prostate. Phys Med Biol. 2002; 47:823–838. [PubMed: 11931473]
22. Rouviere O, Papillard M, Girouin N, Boutier R, Rabilloud M, Riche B, Mege-Lechevallier F, Colombel M, Gelet A. Is it possible to model the risk of malignancy of focal abnormalities found at prostate multiparametric MRI? Eur Radiol. 2012; 22:1149–1157. [PubMed: 22227613]
23. Vos PC, Hambrock T, Hulsbergen-van de Kaa CA, Futterer JJ, Barentsz JO, Huisman HJ. Computerized analysis of prostate lesions in the peripheral zone using dynamic contrast enhanced MRI. Med Phys. 2008; 35:888–899. [PubMed: 18404925]
24. Groenendaal G, Borren A, Moman MR, Monninkhof E, van Diest PJ, Philippens ME, van Vulpen M, van der Heide UA. Pathologic validation of a model based on diffusion-weighted imaging and

dynamic contrast-enhanced magnetic resonance imaging for tumor delineation in the prostate peripheral zone. Int J Radiat Oncol Biol Phys. 2012; 82:e537–544. [PubMed: 22197085]

25. Langer DL, van der Kwast TH, Evans AJ, Trachtenberg J, Wilson BC, Haider MA. Prostate cancer detection with multi-parametric MRI: logistic regression analysis of quantitative T2, diffusion-weighted imaging, and dynamic contrast-enhanced MRI. J Magn Reson Imaging. 2009; 30:327–334. [PubMed: 19629981]
26. Ozer S, Langer DL, Liu X, Haider MA, van der Kwast TH, Evans AJ, Yang Y, Wernick MN, Yetik IS. Supervised and unsupervised methods for prostate cancer segmentation with multispectral MRI. Med Phys. 2010; 37:1873–1883. [PubMed: 20443509]
27. Viswanath SE, Bloch NB, Chappelow JC, Toth R, Rofsky NM, Genega EM, Lenkinski RE, Madabhushi A. Central gland and peripheral zone prostate tumors have significantly different quantitative imaging signatures on 3 Tesla endorectal, in vivo T2-weighted MR imagery. J Magn Reson Imaging. 2012; 36:213–224. [PubMed: 22337003]
28●●. Shah V, Turkbey B, Mani H, Pang Y, Pohida T, Merino MJ, Pinto PA, Choyke PL, Bernardo M. Decision support system for localizing prostate cancer based on multiparametric magnetic resonance imaging. Med Phys. 2012; 39:4093–4103. The researcers developed a decision support system (DSS) for detecting and localizing peripheral zone prostate cancers by using a machine learning approach to calculate a cancer probability map from mp-MRI. [PubMed: 22830742]
29. Vos PC, Barentsz JO, Karssemeijer N, Huisman HJ. Automatic computer-aided detection of prostate cancer based on multiparametric magnetic resonance image analysis. Phys Med Biol. 2012; 57:1527–1542. [PubMed: 22391091]
30●●. Giannini V, Mazzetti S, Vignati A, Russo F, Bollito E, Porpiglia F, Stasi M, Regge D. A fully automatic computer aided diagnosis system for peripheral zone prostate cancer detection using multi-parametric magnetic resonance imaging. Comput Med Imaging Graph. 2015; 46(Pt 2):219–226. The authors described a pipeline of a computer-aided diagnosis system that is conceived as a two-stage process, i.e. the generation of a malignancy probability map for all voxels within the prostate and a candidate segmentation step for highlighting suspected areas. [PubMed: 26391055]
31●●. Peng Y, Jiang Y, Yang C, Brown JB, Antic T, Sethi I, Schmid-Tannwald C, Giger ML, Eggener SE, Oto A. Quantitative analysis of multiparametric prostate MR images: differentiation between prostate cancer and normal tissue and correlation with Gleason score–a computer-aided diagnosis development study. Radiology. 2013; 267:787–796. The authors evaluated the utility of a number of parameters obtained on T2w, DWI, and DCE-MRI for prostate CAD and the assessment of cancer aggressiveness. Their study shows that the combination of the 10^{th} percentile ADC, average ADC, and T2-weighted skewness yielded a high AUC value and that ADC image features and K(trans) are moderately correlated with the Gleason score. [PubMed: 23392430]
32. Betrouni N, Makni N, Lakroum S, Mordon S, Villers A, Puech P. Computer-aided analysis of prostate multiparametric MR images: an unsupervised fusion-based approach. Int J Comput Assist Radiol Surg. 2015; 10:1515–1526. [PubMed: 25605298]
33. Litjens G, Debats O, Barentsz J, Karssemeijer N, Huisman H. Computer-aided detection of prostate cancer in MRI. IEEE Trans Med Imaging. 2014; 33:1083–1092. [PubMed: 24770913]
34. Niaf E, Rouviere O, Mege-Lechevallier F, Bratan F, Lartizien C. Computer-aided diagnosis of prostate cancer in the peripheral zone using multiparametric MRI. Phys Med Biol. 2012; 57:3833–3851. [PubMed: 22640958]
35●. Kwak JT, Xu S, Wood BJ, Turkbey B, Choyke PL, Pinto PA, Wang S, Summers RM. Automated prostate cancer detection using T2-weighted and high-b-value diffusion-weighted magnetic resonance imaging. Med Phys. 2015; 42:2368–2378. The authors proposed a CAD system for prostate cancer to aid in improving the accuracy, reproducibility, and standardization of mp-MRI. The system utilizes T2w MRI and DWI and texture features based on local binary patterns. [PubMed: 25979032]
36●. Vos PC, Hambrock T, Barenstz JO, Huisman HJ. Computer-assisted analysis of peripheral zone prostate lesions using T2-weighted and dynamic contrast enhanced T1-weighted MRI. Phys Med Biol. 2010; 55:1719–1734. The researchers presented an approach for computer-assisted analysis of prostate lesions by combining information from T2w and DCE T1-w MRI. Their study demonstrated a simple T2 estimation method that has a diagnostic performance such that it

complements a DCE T1-w-based CADx system in discriminating malignant lesions from normal and benign regions. [PubMed: 20197602]

37●. Rampun A, Zheng L, Malcolm P, Tiddeman B, Zwiggelaar R. Computer-aided detection of prostate cancer in T2-weighted MRI within the peripheral zone. Phys Med Biol. 2016; 61:4796–4825. The authors reported a prostate CAD system based on T2w MRI and suggested a set of discriminant texture descriptors extracted from T2w MRI data from which 215 texture descriptors were extracted and 11, different classifiers were used to achieve the optimal results. [PubMed: 27272935]

38. Zhao K, Wang C, Hu J, Yang X, Wang H, Li F, Zhang X, Zhang J, Wang X. Prostate cancer identification: quantitative analysis of T2-weighted MR images based on a back propagation artificial neural network model. Sci China Life Sci. 2015; 58:666–673. [PubMed: 26025283]

39. Sung YS, Kwon HJ, Park BW, Cho G, Lee CK, Cho KS, Kim JK. Prostate cancer detection on dynamic contrast-enhanced MRI: computer-aided diagnosis versus single perfusion parameter maps. AJR Am J Roentgenol. 2011; 197:1122–1129. [PubMed: 22021504]

40. Puech P, Betrouni N, Makni N, Dewalle AS, Villers A, Lemaitre L. Computer-assisted diagnosis of prostate cancer using DCE-MRI data: design, implementation and preliminary results. Int J Comput Assist Radiol Surg. 2009; 4:1–10.

41. Matulewicz L, Jansen JF, Bokacheva L, Vargas HA, Akin O, Fine SW, Shukla-Dave A, Eastham JA, Hricak H, Koutcher JA, et al. Anatomic segmentation improves prostate cancer detection with artificial neural networks analysis of 1H magnetic resonance spectroscopic imaging. J Magn Reson Imaging. 2014; 40:1414–1421. [PubMed: 24243554]

42●●. Giannini V, Mazzetti S, Armando E, Carabalona S, Russo F, Giacobbe A, Muto G, Regge D. Multiparametric magnetic resonance imaging of the prostate with computer-aided detection: experienced observer performance study. Eur Radiol. 2017 The researchers compared the performance of experienced readers for detecting prostate cancer using likelihood maps generated by a CAD system with that of the unassisted interpretation of mp-MRI. Their study study demonstrated that with CAD, the sensitivity increases and that CAD significantly reduces the reporting time of mp-MRI.

43●●. Niaf E, Lartizien C, Bratan F, Roche L, Rabilloud M, Mege-Lechevallier F, Rouviere O. Prostate focal peripheral zone lesions: characterization at multiparametric MR imaging–influence of a computer-aided diagnosis system. Radiology. 2014; 271:761–769. Their study assessed the impact of a CAD system on the characterization of focal prostate lesions using mp-MRI. The authors demonstrated that a CAD system improves the characterization of prostate lesions on mp-MRI by increasing the reading specificity. [PubMed: 24592959]

44●●. Hambrock T, Vos PC, Hulsbergen-van de Kaa CA, Barentsz JO, Huisman HJ. Prostate cancer: computer-aided diagnosis with multiparametric 3-T MR imaging–effect on observer performance. Radiology. 2013; 266:521–530. The resarchers investigated the effect of CAD on both less and more clinically experienced observer performance in the differentiation of benign from malignant prostate lesions using mp-MRI. Their study demonstrated that the addition of CAD significantly improved the performance of less clinically experienced observers for distinguishing benign from malignant lesions; when less clinically experienced observers used CAD, they achieved similar clinical performance to that of clinically experienced observers. [PubMed: 23204542]

45●●. Litjens GJ, Barentsz JO, Karssemeijer N, Huisman HJ. Clinical evaluation of a computer-aided diagnosis system for determining cancer aggressiveness in prostate MRI. Eur Radiol. 2015; 25:3187–3199. The authors investigated the added value of CAD on the diagnostic accuracy of PI-RADS reporting and the assessment of cancer aggressiveness. This study demonstrated that i) CAD helps radiologists to discriminate benign findings from cancer using prostate MRI, ii) Combining PI-RADS and CAD improves the differentiation between indolent and aggressive cancer, and iii) Adding CAD to PI-RADS increases the correlation coefficient with respect to the cancer grade. [PubMed: 26060063]

46. Viswanath S, Bloch BN, Chappelow J, Patel P, Rofsky N, Lenkinski R, Genega E, Madabhushi A. Enhanced Multi-Protocol Analysis via Intelligent Supervised Embedding (EMPrAvISE): Detecting Prostate Cancer on Multi-Parametric MRI. Proc SPIE Int Soc Opt Eng. 2011; 7963:79630U.

47. Tiwari P, Kurhanewicz J, Madabhushi A. Multi-kernel graph embedding for detection, Gleason grading of prostate cancer via MRI/MRS. Med Image Anal. 2013; 17:219–235. [PubMed: 23294985]

48. Dinh CV, Steenbergen P, Ghobadi G, Heijmink SW, Pos FJ, Haustermans K, van der Heide UA. Magnetic resonance imaging for prostate cancer radiotherapy. Phys Med. 2016; 32:446–451. [PubMed: 26858164]

49. Litjens GJS, Elliott R, Shih N, Feldman M, Barentsz JO, Hulsbergen - van de Kaa CA, Kovacs I, Huisman HJ, Madabhushi A. Distinguishing prostate cancer from benign confounders via a cascaded classifier on multi-parametric MRI. 2014 903512-903512-903514.

- Multi-parametric MRI has an increasing role in the diagnosis of prostate cancer.
- Computer-aided diagnosis (CAD) of prostate cancer with MRI can improve sensitivity.
- CAD of prostate cancer with MRI was able to improve the specificity.
- CAD can help less clinically experienced readers.
- CAD may help to make a clinical decision in a fast, effective, and reliable way.

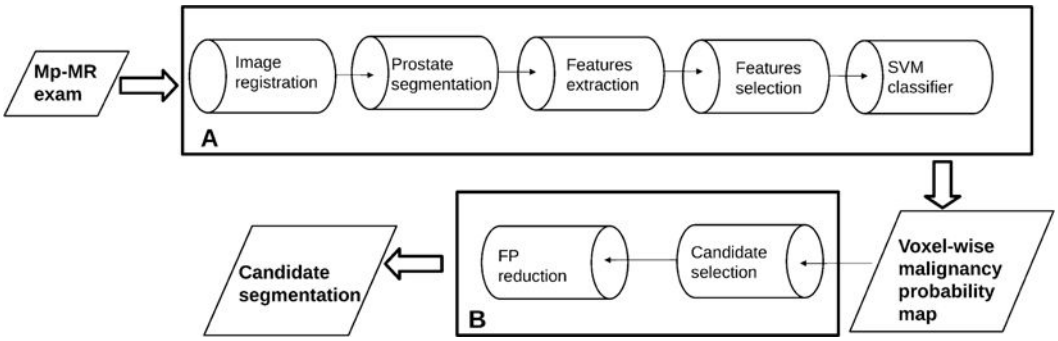

Figure 1.

Flowchart of the CAD system by Giannini *et al.* [30]. Box A represents the steps that are necessary to create the voxel-wise malignancy probability map, while box B represents the candidate segmentation steps.

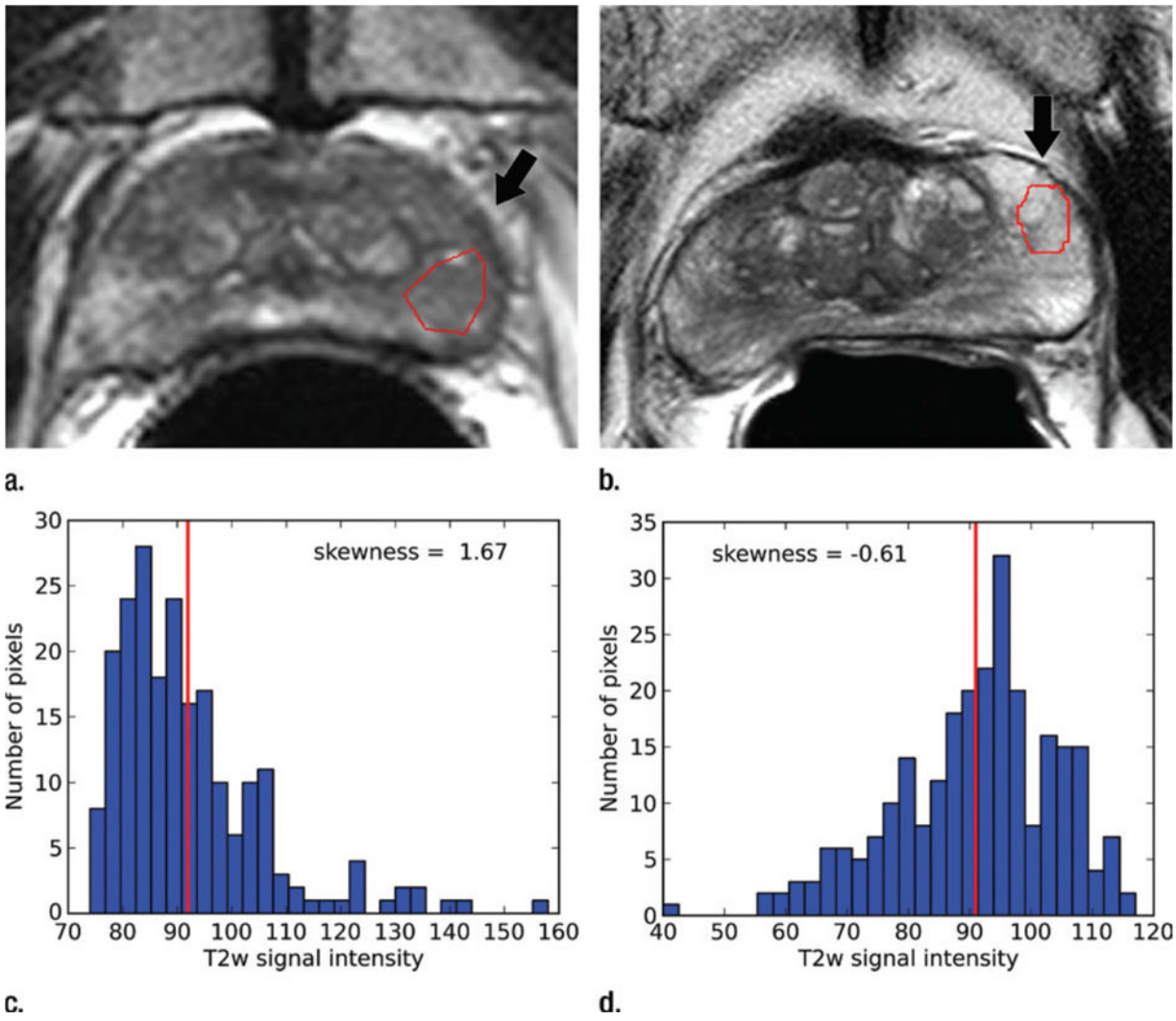

Figure 2.

T2-weighted MR images show (a) a tumor (arrow) in a 66-year-old man with a GS of 7 (4+3) and a prostate-specific antigen level of 13.02 ng/mL and (b) an area of PZ normal tissue (arrow) in a 64-year-old man with prostate cancer elsewhere. Red outlines indicate ROIs. (c, d) Corresponding histograms show T2-weighted signal intensities within the ROIs and the corresponding skewness image feature values. The tumor ROI has more dark pixels than bright pixels, whereas the normal tissue ROI has more bright pixels than dark pixels. Red lines in c and d identify the average, T2-weighted signal intensity within each ROI.

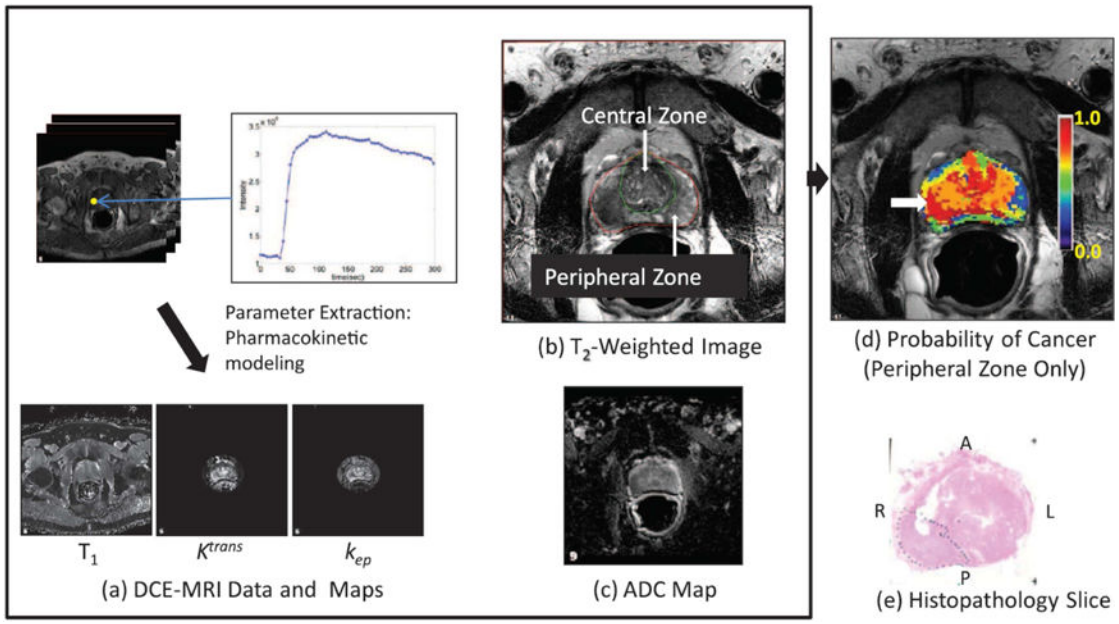

Figure 3.

Illustration of the computer-aided, decision support system. Multiparametric MRI images (a)–(c), resulting in a color–coded, cancer probability map (d) superimposed on a T2W image with a white arrow indicating the region of highest probability, and a histopathology slide (e) confirming the presence of tumor (Gleason score 3 +4, dotted line) in the region with the highest probability. The anterior (A), posterior (P), left (L), and right (R) sides are labeled.